Article

Discovery Medicine 2023; 35(178): 853–860
https://doi.org/10.24976/Discov.Med.202335178.80

Semaglutide Pretreatment Induces Cardiac Autophagy to Reduce Myocardial Injury in Septic Mice

Wei Zhang[1], Jianjian Zhang[2,*]

[1]Intensive Care Unit, Shandong Provincial Third Hospital, Cheeloo College of Medicine, Shandong University, 250031 Jinan, Shandong, China
[2]Department of Endocrinology, Jinan 2nd People's Hospital, 250022 Jinan, Shandong, China
*Correspondence: zhangjianjian0726@outlook.com (Jianjian Zhang)
Published: 1 October 2023

Background: Sepsis-induced myocardial dysfunction (SIMD) confers substantial morbidity and mortality. Semaglutide treatment has demonstrated efficacy in ameliorating sepsis-related organ damage via attenuation of inflammation, oxidative stress, and apoptotic cell death. In this study, we constructed a mouse SIMD model using cecal ligation and puncture (CLP) to explore whether semaglutide preconditioning can modulate autophagy levels and attenuate myocardial injury.

Methods: C57BL/6 mice were randomly divided into six groups: sham, CLP (including CLP-6 h, CLP-12 h and CLP-24 h subgroups), semaglutide, and semaglutide+Compound-C, with five mice in each group. The latter two groups were given daily intraperitoneal injections of semaglutide for 14 days. The semaglutide+Compound-C group was given the autophagy inhibitor Compound-C intraperitoneally 1-hour before CLP surgery. After the last injection of semaglutide, SIMD mouse models were constructed by CLP surgery, while the sham group underwent a sham operation. All mice were sacrificed after surgery, and blood and myocardial specimens were collected. Enzyme-linked immunosorbent assay (ELISA) was used to measure the levels of inflammatory factors and myocardial injury markers in the serum, while quantitative real-time polymerase chain reaction (qRT-PCR) and western blot was used to detect the expression of autophagic markers [microtubule-associated protein 1A/1B-light chain 3B (LC3B), Beclin-1, p62] and AMP-activated protein kinase (AMPK) in myocardial tissue. Hematoxylin and eosin (H&E) staining was used to observe pathological changes in myocardial tissue.

Results: The myocardial fibers in the sham group were normal, while those in the CLP group showed disordered arrangement, interstitial edema, and a large number of infiltrating inflammatory cells. A few vacuolar changes were observed locally in the semaglutide group, and more vacuolar changes were observed in the semaglutide+Compound-C group. Autophagy was inhibited in the CLP group mice. Compared with the CLP group, the semaglutide group showed a decreased levels of inflammatory factors (tumor necrosis factor-α, interleukin-1β) and myocardial injury markers (creatine kinase isoenzyme, cardiac troponin T) in the serum, a reduced expression of autophgic substrate p62, and an increased expression of LC3II (the lipidated form of LC3I)/LC3I (microtubule-associated protein 1A/1B-light chain 3), Beclin-1, and p-AMPK (phosphorylated AMP-activated protein kinase)/AMPK in the injured myocardial tissues of mice ($p < 0.05$). And the protective effects of semaglutide against SIMD were partially reversed by the treatment of AMPK inhibitor Compound-C ($p < 0.05$).

Conclusions: Taken together, these data indicate that semaglutide provides protection against CLP-triggered myocardial inflammation and injury, potentially by reactivating myocardial autophagy pathways via activation of AMPK signaling. Further mechanistic studies are needed to definitively elucidate the functional significance of AMPK signaling in mediating the beneficial cardiac effects of semaglutide during sepsis.

Keywords: semaglutide; myocardial injury; sepsis; autophagy; inflammation

Introduction

Sepsis refers to life-threatening organ dysfunction caused by a dysregulated immune response to infection. The heart is commonly affected, as 40–50% of septic patients develop myocardial injury and dysfunction. Sepsis-induced myocardial dysfunction (SIMD) carries a mortality rate as high as 70–90%, underscoring the need for effective therapies [1–3]. The pathogenesis of SIMD remains incompletely understood but likely involves microcirculatory disturbances, inflammation, autophagy impairment, oxidative stress, and mitochondrial dysfunction.

Autophagy constitutes a homeostatic mechanism by which cells engulf and degrade damaged constituents via lysosomal machinery, thereby maintaining cellular integrity [4]. Optimal levels of autophagic flux are considered cytoprotective in sepsis pathogenesis. However, autophagic processes are notably impaired in septic organisms. Therefore, restoring physiological autophagy may represent a promising strategy to mitigate SIMD [5–7].

Semaglutide, an anti-diabetic glucagon-like peptide-1 analog, has shown protective effects against organ injury in sepsis models by reducing inflammation and oxidative

stress [8]. Stimulation of AMP-activated protein kinase (AMPK) has been implicated as an underlying mechanism for semaglutide's therapeutic effects [9]. Semaglutide can phosphorylate and activate AMPK, which directly stimulates autophagosome formation via Unc-51-like kinase 1 (ULK1) phosphorylation [10,11]. While semaglutide mitigates obesity-induced myocardial injury [12], its effects on sepsis-induced cardiac damage remain unknown.

In this study, we constructed a mouse SIMD model using cecal ligation and puncture (CLP) [13] to explore whether semaglutide preconditioning can modulate autophagy levels and attenuate myocardial injury. This may provide insight into semaglutide's therapeutic potential for SIMD by elucidating underlying mechanisms. Understanding semaglutide's cardioprotective actions will facilitate its development as a novel pharmacologic strategy against SIMD and associated mortality in sepsis.

Materials and Methods

Antibodies, Drugs and Reagents

Semaglutide was obtained from Novo Nordisk (Cat #NDC 0169-4524-14, Bagsværd, Denmark). Compound-C (Cat #171260) was obtained from SigmaAldrich (Shanghai, China). The assay kits detecting cardiac troponin T (cTnT; Cat #EEL112), creatine kinase isoenzyme (CK-MB; Cat #NBP275312), tumor necrosis factor-α (TNF-α; Cat #88-7324-88) and interleukin-1β (IL-1β; Cat #88-7013-22) were purchased from ThermoFisher Scientific (Waltham, MA, USA). The antibodies against microtubule-associated protein 1A/1B-light chain 3B (LC3B; Cat #PA5-32254), Beclin-1 (Cat #PA1-16857), p62 (Cat #PA5-27800), AMPK threonine 172 (Thr172) phosphorylation (p-AMPK; Cat #PA5-37821), AMPK (Cat #PA5-105297), glyceraldehyde 3-phosphate dehydrogenase (GAPDH; Cat #PA1-988), and horseradish peroxidase (HRP)-conjugated goat anti-rabbit secondary antibody (Cat #31460) were purchased from ThermoFisher Scientific (Waltham, MA, USA).

Establishment of SIMD Mice

This study was approved by the Animal Committee of Shandong University (No. 2022-1288). The study utilized male C57BL/6 mice of SPF grade, aged 6–8 weeks, with a body weight of (20 $\pm$ 3) g. The mice were housed in the animal facility of Shandong Provincial Third Hospital, under a 12-hour light/dark cycle and with *ad libitum* access to food and water. The mice were randomly divided into six groups: sham, CLP-6 h (6-hour), CLP-12 h, CLP-24 h, semaglutide and semaglutide+Compound-C, with five mice in each group.

The sham and CLP (including CLP-6 h, CLP-12 h and CLP-24 h) groups received intraperitoneal injections of saline. In contrast, the semaglutide group received semaglutide (30 nmol/kg [8,12], which was suggested by previous research) via intraperitoneal injection at a fixed time daily (4:00 PM) for 14 consecutive days. CLP modeling (CLP-24 h) was performed on the mice 24-hour after the last injection of metformin. The semaglutide+Compound-C group received an intraperitoneal injection of Compound-C (10 mg/kg, which was suggested by previous research [14]) 1-hour prior to CLP surgery (CLP-24 h), while the remaining groups received injections of saline.

The SIMD mouse model was established following the cecal ligation and puncture (CLP) procedure reported in prior studies [13]. Prior to the CLP surgery, all mice were fasted for 12-hour and water was withheld for 6-hour. Each mouse was given an intraperitoneal injection of 2% sodium pentobarbital (50 mg/kg) in the lower right abdomen. Once satisfactory anesthesia was achieved, the mice were fixed in the supine position. The surgical site was prepared with routine skin preparation, sterilization, and draping. A vertical incision about 1cm long was made 0.5 cm to the left of the midline of the abdomen. The peritoneum was bluntly separated to locate the cecum. The length of the cecum was measured with a ruler, and the middle portion of the cecum, located halfway from the blind end, was tied off. Avoiding the blood vessels, a 22-gauge needle was used to puncture the tied-off section twice, gently squeezing out a small amount of intestinal content. The cecum was then returned to the abdomen and the incision was sutured layer by layer. Postoperatively, 1 mL of warm (37 °C) saline was injected subcutaneously in the nape of the neck for fluid resuscitation. The mice were then returned to separate cages in the animal room and allowed free access to food and water once they had recovered from anesthesia. The sham group underwent the same procedure, except for the cecal ligation and puncture. Blood samples were collected from the sham group-24-hour postoperatively and from the CLP (including CLP-6 h, CLP-12 h and CLP-24 h), semaglutide and semaglutide+Compound-C groups at the corresponding postoperative times using the eye removal method, after anesthetizing the mice. Once blood collection was complete, the mice were euthanized using cervical dislocation, and the hearts were harvested immediately for subsequent experiments.

Enzyme-Linked Immunosorbent Assay (ELISA)

The whole blood collected from each group of mice were centrifuged at 4 °C and 3000 rpm for 20-minute to obtain serum. The serum samples were then subjected to ELISA by adding reagents (cTnT, CK-MB, TNF-α and IL-1β) according to the instructions of the assay kit, and the corresponding absorbance (450 nm) was measured using ultraviolet-visible spectroscopy (UV-1900i, Shimadzu, Kyoto, Japan).

Hematoxylin and Eosin (H&E) Staining

After euthanizing the mice, the myocardial tissue collected from each group of mice with the largest transverse diameter in the coronal plane of the left ventricle was ex-

Table 1. Primers used for qRT-PCR.

Gene symbol	Forward primer (5′ → 3′)	Reverse primer (5′ → 3′)
18s rRNA	GATGGGAAGTACAGCCAGGT	TTTCTTCAGCCTCTCCAGGT
microtubule-associated protein 1A/1B-light chain 3B (LC3B)	CAGGCTTTCGTCTCTTCCACCATC	CCAGGACAAGCAGGCAGATGAAG

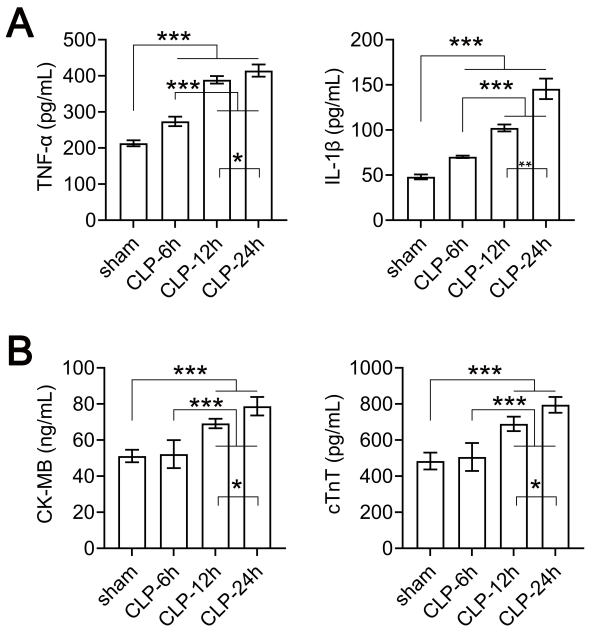

Fig. 1. Expression of serum inflammatory cytokines and myocardial injury markers in sham versus CLP (cecal ligation and puncture) mice. (A) Serum levels of the inflammatory factors TNF-α (tumor necrosis factor-α) and IL-1β (interleukin-1β) in sham, CLP-6 h, CLP-12 h, and CLP-24 h groups. (B) Serum levels of the myocardial injury markers CK-MB (creatine kinase isoenzyme) and cTnT (cardiac troponin T) in sham, CLP-6 h, CLP-12 h, and CLP-24 h groups. *$p < 0.05$, **$p < 0.01$, ***$p < 0.001$.

tracted and fixed in 10% neutral buffered formalin solution at a volume ratio of 1:10 for preservation. Following embedding, tissue sections with a thickness of 0.5 µm were prepared. The sections were then stained with H&E staining and evaluated for histopathological evaluation of myocardial tissue alterations under the BX61 microscope (BX61, Olympus, Tokyo, Japan) in three randomly selected fields by two pathologists in a blinded manner.

Quantitative Real-Time Polymerase Chain Reaction (qRT-PCR)

Total RNA was extracted from the myocardial tissues from each group of mice using TRIzol reagent (Cat #15596026, ThermoFisher, Waltham, MA, USA). The cDNA was synthesized from 1 µg of total RNA using the TaKaRa RNA PCR Kit (Cat #RR019, Takara, Shiga, Japan). The qRT-PCR was performed with the TaqMan fluorogenic PCR system (Cat #TP950, Takara, Shiga, Japan). qRT-PCR was performed using 18S ribosomal RNA (18S rRNA) as an internal reference gene for normalization. After amplification, the Ct values of each group were recorded, and the relative gene expression was evaluated using the $2^{-\Delta\Delta Ct}$ method. The primer sequences were listed in Table 1.

Western Blot Analysis

The myocardial tissues collected from each group of mice were lysed with NE-PER™ nuclear and cytoplasmic extraction reagents (Cat #78833, ThermoFisher Scientific, Waltham, MA, USA) and complete protease inhibitor (Cat #11697498001, Roche, Basel, Switzerland) on ice. The protein concentrations were tested using the Bicinchoninic Acid Protein Assay Kit (Cat #23225, ThermoFisher Scientific, Waltham, MA, USA). For western blot analysis, 30 µg of protein from each sample was applied for sodium dodecyl-sulfate polyacrylamide gel electrophoresis. After separation, the proteins were transferred into polyvinylidene difluoride (PVDF) membranes (Cat #88518, ThermoFisher Scientific, Waltham, MA, USA). The PVDF membranes were blocked with 5% nonfat dry milk for nearly 1-hour and then incubated with the primary antibodies at 4 °C for about 24-hour. The following primary antibodies were used: anti-LC3B (1:200), anti-Beclin-1 (1:400), anti-p62 (1:500), anti-p-AMPK (1:200), anti-AMPK (1:500), anti-GAPDH (1:10,000). This was followed by the incubation with the HRP-conjugated goat anti-rabbit secondary antibody (1:5000) at room temperature for nearly 1-hour. Protein bands were visualized using BeyoECL Moon (Cat #P0018FS, Beyotime, Shanghai, China). The band densities of western blot analysis were quantified by the ImageJ V2.0.0 software (National Institutes of Health, Bethesda, MD, USA), and the relative protein levels were calculated based on GAPDH as the loading control.

Statistical Analysis

Statistical analysis was performed using GraphPad Prism 8.0 software (GraphPad Software, San Diego, CA, USA). Data normality was determined by using Shapiro-Wilkes test. Differences ($p < 0.05$ considered significant) between two independent samples with normal distribution were determined by using Student's *t*-test, while Mann-Whitney test was used to compare non-normal data ($p < 0.05$ considered significant). For more than two normally distributed samples, statistical comparisons were made by

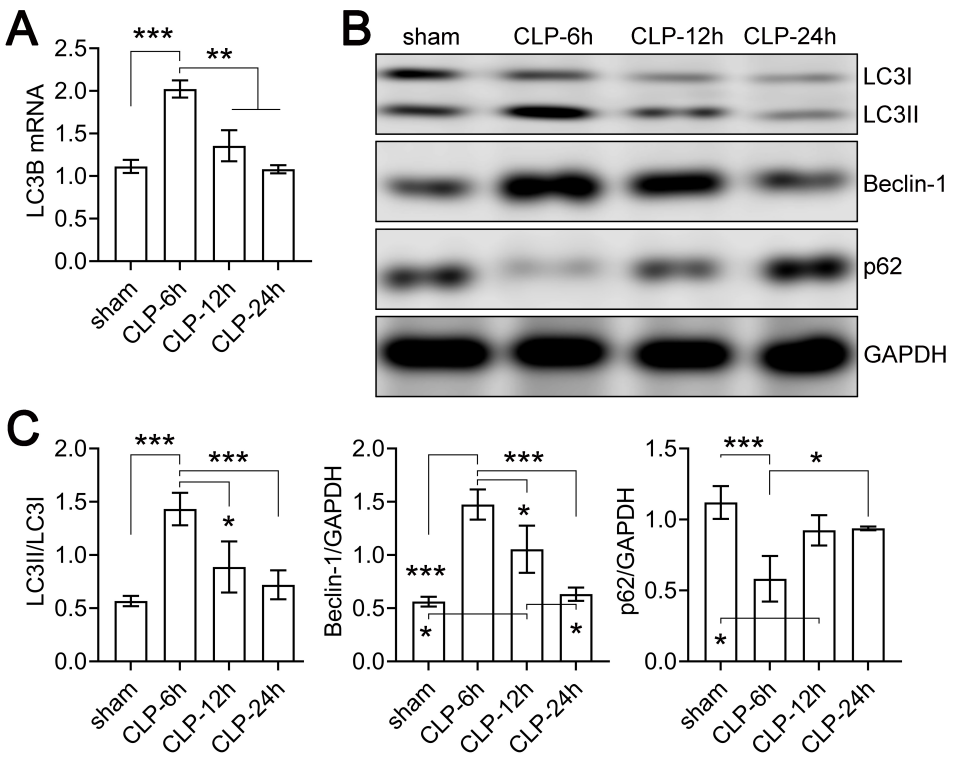

Fig. 2. Autophagy marker expression in myocardial tissue of sham versus CLP mice. (A) LC3B mRNA levels in sham, CLP-6 h, CLP-12 h, and CLP-24 h groups measured by quantitative RT-PCR. (B) Representative western blots showing LC3I (microtubule-associated protein 1A/1B-light chain 3), LC3II (the lipidated form of LC3I), Beclin-1, and p62 protein levels in sham and CLP groups. GAPDH (glyceraldehyde 3-phosphate dehydrogenase) was used as loading control. (C) Densitometric quantification of LC3II/LC3I ratio, Beclin-1, and p62 protein expression normalized to GAPDH. Data represent mean ± SD. *$p < 0.05$, **$p < 0.01$, ***$p < 0.001$.

one-way analysis of variance (ANOVA) with Tukey's range test. An adjusted $p < 0.05$ was considered significant after Tukey's or Benjamini-Hochberg corrections for multiple comparisons.

Results

The Construction of SIMD Mice

Serum levels of the inflammatory cytokines TNF-α and IL-1β, as well as the myocardial injury markers CK-MB and cTnT [15,16], were quantified by ELISA in sham and CLP groups (Fig. 1A,B). Compared to sham, all CLP groups displayed significantly elevated TNF-α and IL-1β levels, with levels highest in the CLP-24 h group. CK-MB and cTnT were markedly higher in the CLP-12 h and CLP-24 h groups versus sham, with levels again highest in CLP-24 h. No significant differences were observed between CLP-6 h and sham, indicating successful establishment of myocardial injury beginning at 12-hour post-CLP, with injury further exacerbated by 24-hour.

Myocardial mRNA and protein levels of autophagy markers were assessed by quantitative real-time PCR (qRT-PCR) and western blotting, respectively (Fig. 2). LC3B mRNA expression and the LC3II (the lipidated form of LC3I)/LC3I (microtubule-associated protein 1A/1B-light chain 3) ratio and Beclin-1 protein levels were significantly higher in the CLP-6 h group compared to sham, but gradually declined to baseline levels by 24-hour post-CLP. Conversely, the autophagic substrate p62 protein was markedly lower at 6-hour before recovering to sham levels by 24-hour. No significant differences in autophagy markers were detected between the CLP-24 h and sham groups. Collectively, these data demonstrate initial autophagy induction at early sepsis stages followed by inhibition upon development of myocardial injury.

Given that autophagy was maximally suppressed at 24-hour post-CLP, when myocardial damage peaked compared to 12-hour (Figs. 1,2), this time point (24-hour post-CLP) was selected for subsequent mechanistic analyses.

The Protective Effect of Semaglutide on Septic Myocardial Injury was Associated with AMPK-Induced Autophagy in SIMD Mice

Compared to the CLP-24 h group, semaglutide pretreatment significantly reduced serum levels of the inflammatory cytokines TNF-α and IL-1β, as well as the myocardial injury markers CK-MB and cTnT, in septic mice (Fig. 3A,B). Furthermore, the autophagy markers LC3II/LC3I and Beclin-1 were markedly upregulated, while p62 was downregulated, in myocardial tissues of

semaglutide-treated versus CLP-24 h mice (Fig. 4A,B). These results provide evidence that semaglutide can enhance protective autophagy in the myocardial tissue of mice with SIMD.

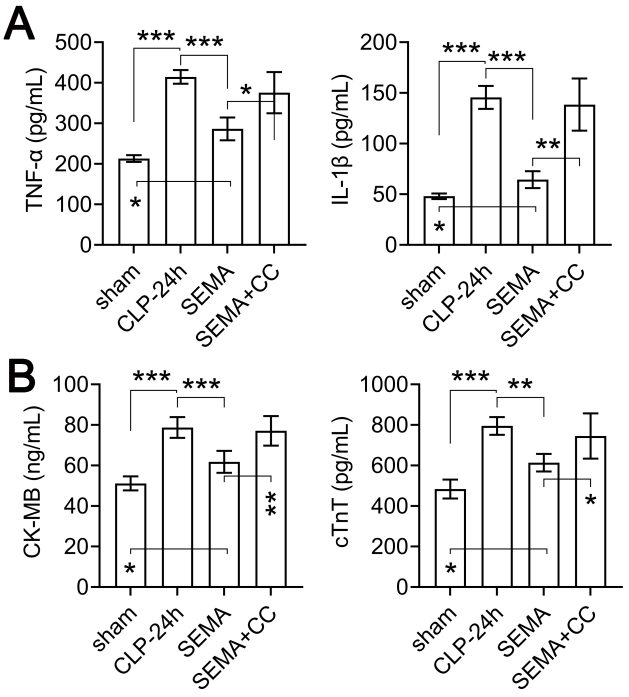

Fig. 3. Expression of serum inflammatory cytokines and cardiac injury markers in sham, CLP-24 h, semaglutide, and semaglutide+Compound-C groups. (A) Levels of the inflammatory factors TNF-α and IL-1β. (B) Levels of the myocardial injury markers CK-MB and cTnT. SEMA refers to the group of mice treated with semaglutide (SEMA). SEMA+CC, refers to the group of mice treated with both semaglutide (SEMA) and Compound C (CC). Data represent mean $\pm$ SD. *$p < 0.05$, **$p < 0.01$, ***$p < 0.001$.

AMPK coordinates stimulation of autophagy through multiple mechanisms [10,11]. We found the ratio of phosphorylated to total AMPK (p-AMPK/AMPK) was significantly increased by semaglutide compared to CLP-24 h controls (Fig. 4C,D), indicating AMPK activation. Furthermore, the AMPK inhibitor Compound-C [14,17,18] markedly suppressed autophagy induction by semaglutide, as evidenced by decreased LC3II/LC3I and Beclin-1 levels and increased p62 levels (Fig. 4A,B). Administration of Compound-C also partially reversed the protective effects of semaglutide against inflammation and myocardial injury markers (Fig. 3A,B).

Representative H&E-Stained Myocardial Samples from Sham, CLP-24 h, Semaglutide, and Semaglutide+Compound-C Groups were Evaluated to Assess Histopathology

Histopathological examination of myocardial tissues from sham, CLP-24 h, semaglutide, and semaglutide+Compound C groups was conducted using H&E staining (Fig. 5). Sham group sections exhibited intact myocardial fibers with no evident damage or immune cell infiltration under light microscopy. CLP-24 h group sections displayed disturbed myofiber arrangement, interstitial edema, erythrocyte extravasation, and abundant infiltrating inflammatory cells. As anticipated, the semaglutide group sections showed only mild edema and localized vacuolar changes in myocardial fibers. However, semaglutide+Compound-C group sections exhibited slightly disordered fibers and substantially increased vacuolization compared to semaglutide alone. These findings suggest semaglutide pretreatment confers some degree of protection against sepsis-induced myocardial tissue injury, which is partially reversed by AMPK inhibition via Compound-C. Further mechanistic studies are warranted to definitively establish the role of AMPK-mediated autophagy in semaglutide's cardioprotective effects during sepsis.

Discussion

Sepsis remains a significant global health challenge characterized by substantial morbidity and mortality [1–3]. Early detection, timely intervention, and preventing complications are crucial for improving outcomes in sepsis patients [1]. Myocardial dysfunction commonly occurs in sepsis and significantly contributes to mortality [1–3]. However, the pathophysiological mechanisms underlying SIMD are not fully elucidated.

Current evidence indicates SIMD involves excessive inflammation, oxidative stress, impaired autophagy, and other factors triggered by infection [1,3]. Autophagy is a process whereby cells degrade and recycle damaged components to maintain homeostasis [4]. Appropriate autophagy levels reportedly protect against sepsis by eliminating pathogens and clearing damaged organelles. However, autophagy is markedly suppressed in later SIMD stages [7]. Inhibiting autophagy exacerbates cardiomyocyte apoptosis and cardiac injury. Thus, restoring physiological autophagy may represent a promising therapeutic approach for SIMD.

In this study, we utilized a mouse CLP model to characterize autophagy changes in SIMD. The key autophagy markers LC3II/LC3I and Beclin-1 [19,20] were significantly elevated at 6-hour post-CLP versus sham controls, but decreased to baseline by 24-hour. Conversely, the autophagy substrate p62 markedly decreased at 6-hour but recovered by 24-hour. These results demonstrate autophagy is initially activated but subsequently inhibited as SIMD progresses, consistent with previous reports [7].

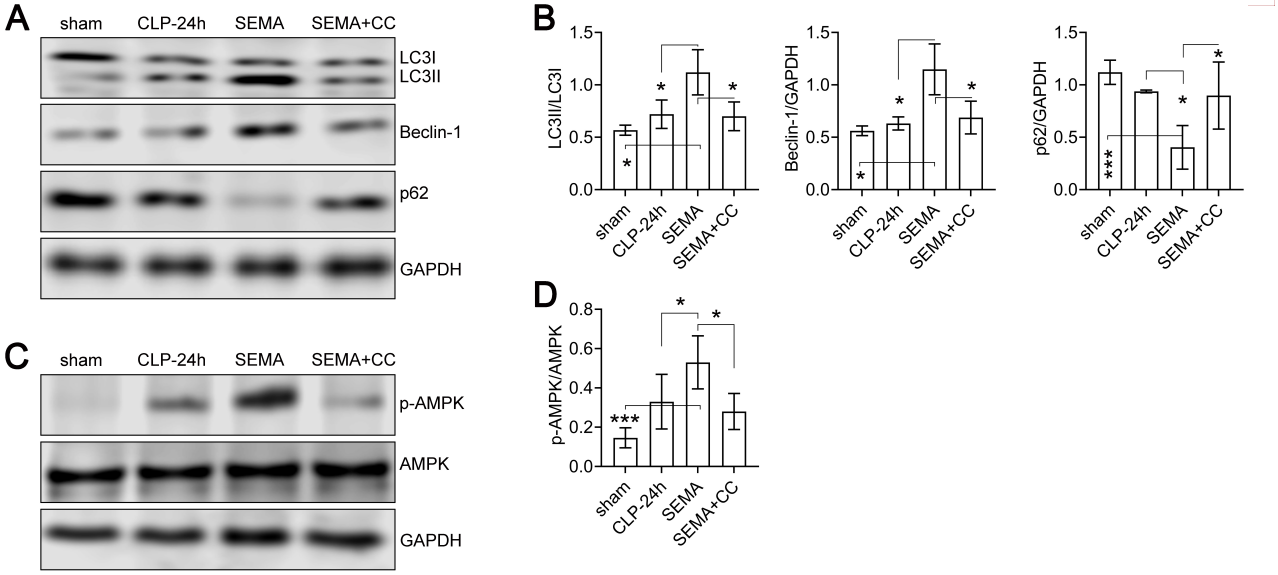

Fig. 4. Autophagy and AMPK (AMP-activated protein kinase) marker expression in myocardial tissue of sham, CLP-24 h, semaglutide, and semaglutide+Compound-C groups. (A) Representative western blots showing LC3I, LC3II, Beclin-1, and p62 protein levels. GAPDH was used as loading control. (B) Densitometric quantification of LC3II/LC3I ratio, Beclin-1, and p62 normalized to GAPDH. (C) Representative western blots showing p-AMPK and total AMPK levels. GAPDH was used as loading control. (D) Densitometric quantification of p-AMPK/AMPK ratio normalized to GAPDH. SEMA, semaglutide group mice; SEMA+CC, semaglutide+Compound-C group mice; p-AMPK, AMPK Thr172 (threonine 172) phosphorylation. Data represent mean ± SD. *$p < 0.05$, ***$p < 0.001$.

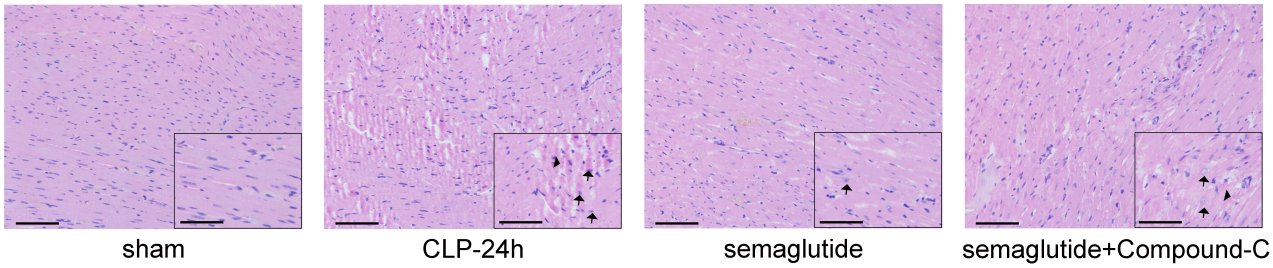

Fig. 5. Representative histopathological changes in myocardial tissues of sham, CLP-24 h, semaglutide, and semaglutide+Compound-C groups. H&E (hematoxylin and eosin) stained sections of myocardial tissue from each group. Arrowheads indicate ruptured myocardial fibers and interstitial edema. Arrows show infiltrated neutrophils. The large image is shown at 10× magnification (Scale bar: 25 μm), while the inset depicts a 40× (Scale bar: 100 μm) magnified view.

Semaglutide, a front-line type 2 diabetes medication, also mitigates sepsis-induced organ injury by modulating inflammation and oxidative stress. Autophagy activation importantly mediates semaglutide's pharmacological effects [21,22]. While semaglutide alleviates cardiomyocyte injury related to obesity via anti-inflammatory actions [12], its impacts on septic cardiac damage were previously unknown. Here, we found LC3II/LC3I and Beclin-1 levels were higher, while p62 was lower, in semaglutide-treated CLP mice versus CLP controls. Serum markers of myocardial injury and inflammation were also reduced with semaglutide treatment. Histology revealed attenuated immune cell infiltration and myofibril disarray. These results suggest enhanced autophagy may underlie semaglutide's cardioprotective effects in sepsis.

AMPK is a key cellular energy sensor that maintains energy homeostasis during stress [23]. Semaglutide has been shown to exert cardiovascular benefits partly through modulating AMPK [8,9]. In this study, we found the ratio of phosphorylated to total AMPK (p-AMPK/AMPK) was increased with semaglutide treatment in septic mice, indicating AMPK activation may be involved. AMPK can suppress inflammation by inhibiting NF-κB signaling [24,25]. As a classic autophagy regulator, AMPK activates the ULK1 and Beclin-1 proteins to initiate autophagy [10,11]. Therefore, semaglutide may induce cardioprotective autophagy via AMPK. Supporting this possibility, administration of the AMPK inhibitor Compound C [14,17,18] attenuated semaglutide's effects on autophagy markers, inflammation, and cardiac injury. Further genetic validation is still

needed to definitively establish the AMPK-autophagy axis underlying semaglutide's cardiac protective actions in this sepsis model.

Conclusions

In summary, impaired autophagy likely contributes to the progress of SIMD. Semaglutide pretreatment appears to activate AMPK, restore autophagy, and mitigate sepsis-induced myocardial inflammation and damage. Elucidating these mechanisms will facilitate developing semaglutide as a therapeutic strategy against the high morbidity and mortality associated with SIMD.

Availability of Data and Materials

All data generated or analysed during this study are included in this published article.

Author Contributions

Study design: WZ, JJZ. Experiment performance: WZ, JJZ. Data analysis: WZ. Manuscript drafting: WZ, JJZ. Both authors read and approved the final manuscript. Both authors agreed to be accountable for all aspects of the work in ensuring that questions related to the accuracy or integrity of any part of the work are appropriately investigated and resolved.

Ethics Approval and Consent to Participate

All mouse injury models were conducted following the standards of the Animal Welfare Committees of Shandong University in Jinan, China for the housing and care of laboratory animals and were approved by the Animal Committee of Shandong University (No. 2022-1288).

Acknowledgment

Not applicable.

Funding

This research received no external funding.

Conflict of Interest

The authors declare no conflict of interest.

References

[1] Rong J, Tao X, Lin Y, Zheng H, Ning L, Lu HS, *et al*. Loss of Hepatic Angiotensinogen Attenuates Sepsis-Induced Myocardial Dysfunction. Circulation Research. 2021; 129: 547–564.

[2] Khalid N, Patel PD, Alghareeb R, Hussain A, Maheshwari MV. The Effect of Sepsis on Myocardial Function: A Review of Pathophysiology, Diagnostic Criteria, and Treatment. Cureus. 2022; 14: e26178.

[3] Shvilkina T, Shapiro N. Sepsis-Induced myocardial dysfunction: heterogeneity of functional effects and clinical significance. Frontiers in Cardiovascular Medicine. 2023; 10: 1200441.

[4] Aman Y, Schmauck-Medina T, Hansen M, Morimoto RI, Simon AK, Bjedov I, *et al*. Autophagy in healthy aging and disease. Nature Aging. 2021; 1: 634–650.

[5] Yin X, Xin H, Mao S, Wu G, Guo L. The Role of Autophagy in Sepsis: Protection and Injury to Organs. Frontiers in Physiology. 2019; 10: 1071.

[6] Sun Y, Cai Y, Zang QS. Cardiac Autophagy in Sepsis. Cells. 2019; 8: 141.

[7] Sun Y, Yao X, Zhang QJ, Zhu M, Liu ZP, Ci B, *et al*. Beclin-1-Dependent Autophagy Protects the Heart During Sepsis. Circulation. 2018; 138: 2247–2262.

[8] Jiang Z, Tan J, Yuan Y, Shen J, Chen Y. Semaglutide ameliorates lipopolysaccharide-induced acute lung injury through inhibiting HDAC5-mediated activation of NF-κB signaling pathway. Human & Experimental Toxicology. 2022; 41: 9603271221125931.

[9] Li Q, Tuo X, Li B, Deng Z, Qiu Y, Xie H. Semaglutide attenuates excessive exercise-induced myocardial injury through inhibiting oxidative stress and inflammation in rats. Life Sciences. 2020; 250: 117531.

[10] Karabiyik C, Vicinanza M, Son SM, Rubinsztein DC. Glucose starvation induces autophagy via ULK1-mediated activation of PIKfyve in an AMPK-dependent manner. Developmental Cell. 2021; 56: 1961–1975.e5.

[11] Park JM, Lee DH, Kim DH. Redefining the role of AMPK in autophagy and the energy stress response. Nature Communications. 2023; 14: 2994.

[12] Pan X, Yue L, Ban J, Ren L, Chen S. Effects of Semaglutide on Cardiac Protein Expression and Cardiac Function of Obese Mice. Journal of Inflammation Research. 2022; 15: 6409–6425.

[13] Siempos II, Lam HC, Ding Y, Choi ME, Choi AMK, Ryter SW. Cecal ligation and puncture-induced sepsis as a model to study autophagy in mice. Journal of Visualized Experiments. 2014; e51066.

[14] Li S, Chen H, Jiang X, Hu F, Li Y, Xu G. Adeno-associated virus-based caveolin-1 delivery via different routes for the prevention of cholesterol gallstone formation. Lipids in Health and Disease. 2022; 21: 109.

[15] Chaulin AM. Elevation Mechanisms and Diagnostic Consideration of Cardiac Troponins under Conditions Not Associated with Myocardial Infarction. Part 2. Life. 2021; 11: 1175.

[16] Agwa SHA, Elzahwy SS, El Meteini MS, Elghazaly H, Saad M, Abd Elsamee AM, *et al*. ABHD4-Regulating RNA Panel: Novel Biomarkers in Acute Coronary Syndrome Diagnosis. Cells. 2021; 10: 1512.

[17] Ahsan M, Garneau L, Aguer C. The bidirectional relationship between AMPK pathway activation and myokine secretion in skeletal muscle: How it affects energy metabolism. Frontiers in Physiology. 2022; 13: 1040809.

[18] Nakao T, Otaki S, Kominami Y, Watanabe S, Ito M, Aizawa T, *et al*. L-Fucose Suppresses Lipid Accumulation via the AMPK Pathway in 3T3-L1 Adipocytes. Nutrients. 2023; 15: 503.

[19] Debnath J, Gammoh N, Ryan KM. Autophagy and autophagy-related pathways in cancer. Nature Reviews. Molecular Cell Biology. 2023; 24: 560–575.

[20] Hu D, Huo Y, Xue Y, Feng H, Sun W, Wang H, *et al*. Clinical application of autophagy proteins as prognostic biomarkers in colorectal cancer: a meta-analysis. Future Oncology. 2022; 18: 3537–3549.

[21] Liu DX, Zhao CS, Wei XN, Ma YP, Wu JK. Semaglutide Protects against 6-OHDA Toxicity by Enhancing Autophagy and Inhibiting Oxidative Stress. Parkinson's Disease. 2022; 2022: 6813017.

[22] Chang YF, Zhang D, Hu WM, Liu DX, Li L. Semaglutide-mediated protection against Aβ correlated with enhancement of

autophagy and inhibition of apotosis. Journal of Clinical Neuroscience. 2020; 81: 234–239.

[23] Hardie DG, Ross FA, Hawley SA. AMPK: a nutrient and energy sensor that maintains energy homeostasis. Nature Reviews. Molecular Cell Biology. 2012; 13: 251–262.

[24] Xiang HC, Lin LX, Hu XF, Zhu H, Li HP, Zhang RY, *et al*. AMPK activation attenuates inflammatory pain through inhibiting NF-κB activation and IL-1β expression. Journal of Neuroinflammation. 2019; 16: 34.

[25] Salminen A, Hyttinen JMT, Kaarniranta K. AMP-activated protein kinase inhibits NF-κB signaling and inflammation: impact on healthspan and lifespan. Journal of Molecular Medicine. 2011; 89: 667–676.